Geochemistry Geophysics Geosystems G3
AN ELECTRONIC JOURNAL OF THE EARTH SCIENCES
Published by AGU and the Geochemical Society

Article
Volume 2
December 28, 2001
Paper number 2001GC000208
ISSN: 1525-2027

Using ocean margin density to constrain ocean circulation and surface wind strength in the past

Jean Lynch-Stieglitz

Lamont-Doherty Earth Observatory, Department of Earth and Environmental Sciences, Columbia University, Palisades, New York 10964, USA (jean@ldeo.columbia.edu)

[1] **Abstract:** The density structure along the ocean margins carries an integrated imprint of ocean circulation. The difference in pressure between the eastern and western margins of the ocean reflects the net meridional geostrophic transport across the ocean basin. If one assumes that the wind driven circulation is closed in the upper ocean, the wind driven component of the net geostrophic transport is equal in magnitude and opposite in direction to the Ekman transport. The remainder of the net meridional geostrophic transport is the upper branch of the thermohaline meridional overturning circulation. The meridional geostrophic transports calculated using the ocean margin density data collected during World Ocean Circulation Experiment (WOCE) reflect both the wind driven and thermohaline overturning circulations. Density along the ocean margins for times in the past can be estimated from the oxygen isotopic composition of benthic foraminifera. These ocean margin density estimates can then be used to help constrain the shear in the meridional overturning circulation, the strength of zonal surface winds over the oceans, and the resulting wind driven circulation. These data will also provide an important complement to existing paleoceanographic reconstructions of surface conditions and deep water tracer fields which are currently used to constrain models of past ocean circulation.

Keywords: Geostrophic transport; ocean margin; oxygen isotopes; foraminifera.

Index terms: Paleoceanography; general circulation; instruments and techniques.

Received July 27, 2001; **Revised** October 1, 2001; **Accepted** October 2, 2001; **Published** December 28, 2001.

Lynch-Stieglitz, J., Using ocean margin density to constrain ocean circulation and surface wind strength in the past, *Geochem. Geophys. Geosyst.*, *2*, 10.1029/2001GC000208, 2001.

1. Introduction

[2] For almost a century, physical oceanographers have used the distribution of density in the ocean to help quantify ocean circulation. A geostrophic balance is assumed, and velocity can then be calculated from density information using either a measured or assumed velocity at a reference level or by combining the geostrophic balance with other constraints (such as conservation of tracer flow across a section). Recently, we have applied this approach to paleoceanography by using vertical density profiles reconstructed from the oxygen isotopic composition of foraminiferal calcite combined with a reference level to calculate the flow through the Florida straits [*Lynch-Stieglitz et al.*, 1999a, 1999b, 1999c]. At this point, we can only reconstruct the vertical density structure for the past ocean using benthic foraminifera

where the seafloor intersects the upper water column (ocean margins, islands, shallow seamounts). Although planktonic foraminifera calcify at various depths within the upper water column, we have no way to quantitatively reconstruct the depth at which they calcified. The ocean margins thus constitute the largest area in the ocean where the vertical density structure can be reconstructed during the past. In addition, measurements along the ocean margins may be an efficient means for the long-term monitoring of upper ocean flow for the modern ocean. In this paper, we investigate how the density structure on the ocean margins can be used to provide information on both the large-scale meridional overturning of the oceans and the strength of the zonal winds over the oceans.

2. What Determines Cross-Basin Density Contrast and Transport?

[3] In the absence of intervening topography, the difference in pressure between the eastern and western margins of the ocean reflects the net meridional geostrophic transport across the ocean basin. At any given depth, the density difference between the eastern and western margins reflects the vertical shear in this transport at that particular depth. The transport could be calculated from density measurements using the dynamic method by assuming a "level of no motion" or, perhaps more accurately, the depth at which the zonally integrated meridional geostrophic transport switches sign. *Marotzke et al.* [1999] show in a model simulation that below 500 m depth the curvature of the meridional overturning stream function (equivalent to the vertical shear in the meridional transport) is proportional to the east–west density difference, and they suggest that the meridional overturning circulation and heat transport could be monitored by measuring density changes along the ocean margins. Here we will examine how the east–west density difference in the upper ocean reflects both the thermohaline overturning circulation and the portion of the wind driven gyre flow that is in geostrophic balance. We concentrate our discussion on the density contrast and circulation in the upper ocean, since the smaller density contrasts associated with the deep flows are difficult to accurately measure in the geologic record.

[4] The geostrophic method is typically used in physical oceanographic studies to reconstruct a velocity profile using two adjacent density profiles (which give the shear in velocity) and either a velocity measurement at some depth or a designated reference level at which it is assumed that the velocity normal to the section is zero. Many closely spaced density profiles along a section can then be used to reconstruct the spatial structure as well as the net flow through the section. Often the reference level is chosen such that the resulting velocity section satisfies certain constraints (e.g., mass or tracer conservation). While closely spaced density information is necessary for detailed flow information, if there were a constant level of no motion along the section (or a depth at which meridional motions were relatively weak), the net transport would be reflected in the net pressure gradient across the section, which depends only on the vertical profiles at the two sides of the section. Paired density profiles have been used to assess the integrated transport of large-scale ocean currents [*Curry and McCartney*, 2001; *Lynch-Stieglitz et al.*, 1999a, 1999b, 1999c; *Sato and Rossby*, 1995; *Whitworth*, 1983]. However, as long as the density profiles are located at the same latitude, there is no reason why the density contrast across an entire ocean basin cannot also be used to calculate the net geostrophic shear across that latitude above the depth of the highest sill.

[5] In the absence of winds, the density contrast across the upper ocean (top 1000 m or so)

should reflect the upper branch of the meridional overturning associated with the thermohaline circulation, which is largely geostrophic. For example, in the Atlantic Ocean, there is net northward flow of surface and intermediate waters which compensate the export of North Atlantic Deep Water (NADW). There should therefore be denser waters along the western margin than the eastern margin (a net tilt in the thermocline upward to the west) in the Northern Hemisphere. The situation would be reversed (a net tilt of the thermocline upward to the east) in the Southern Hemisphere reflecting the change in sign of the Coriolis parameter. Indeed this is what is seen in data from 30°N and 30°S, where the zonal winds are weak. In the North Pacific, where there is no strong surface to deep overturning cell as in the Atlantic, the thermocline would have no net tilt due to the thermohaline circulation.

[6] However, there is also net geostrophic transport across the ocean basins that is due to the primarily horizontal wind driven circulation. At any given latitude, the net meridional Ekman transport, T_e is proportional to the zonal wind stress:

$$T_e = \frac{-\tau_x}{\rho_0 f} L, \tag{1}$$

where τ_x is average zonal wind stress across the basin, f is the Coriolis parameter, ρ_0 is the density of seawater, and L is the width of the basin. The Ekman transport itself is not reflected in the density structure of the upper ocean and thus does not affect the east–west density contrast. However, the resulting convergence and divergence of surface waters create pressure gradients that induce additional flow, which is to a large extent geostrophically balanced. If one then assumes that the wind driven flow, including both the Ekman transport and the wind driven geostrophic transport (T_{gw}), is closed in the upper ocean (no net wind driven meridional transport across the width of the ocean basin; vertical motions to/from the deep ocean small relative to horizontal motions),

$$T_e + T_{gw} = 0\,. \tag{2}$$

It follows that in the absence of the large-scale thermohaline overturning, the net wind-driven geostrophic transport across the ocean would be equal in magnitude and opposite in direction to the Ekman transport [*Roemmich*, 1983].

[7] The Ekman transport, which takes place in the mixed layer, combined with the subsurface wind-driven geostrophic flow in the opposite direction forms shallow wind-driven overturning cells in the integrated meridional circulation. The subtropical cell consists of the poleward transport of surface waters away from the equator (primarily Ekman transport), subduction of surface water into the thermocline in the subtropical gyre, equatorward flow of thermocline waters (geostrophically balanced), and upwelling of these thermocline waters at the equator [*McCreary and Lu*, 1994]. Although less widely noted, *McCreary and Lu* [1994] also describes a weaker subpolar cell consisting of upwelling in the subpolar gyre, equatorward Ekman transport, subduction in the subtropical gyre, and a poleward subsurface geostrophic flow to close the cell.

[8] Combining (1) and (2) with the fact that the meridional geostrophic transport is proportional to the east–west density gradients divided by the Coriolis parameter, f, (equation (5)), it becomes clear that the net pressure gradients across the upper ocean are directly proportional to the zonal wind stress. In other words, the net east–west tilt of the thermocline due to the wind driven portion of upper ocean flow is proportional to the zonal wind stress at any given latitude, just as it is at the equator. Discussing this phenomenon in a two-layer model, *Veronis* [1981, p. 157] notes that

> the result is exactly the one obtained for a nonrotating lake where the wind blows the

warm water to the leeward edge and causes the thermocline to rise on the windward side. The principal difference between the two phenomena is that the induced pressure gradient drives a vertical circulation in the lake, whereas it is geostrophically balanced in the rotating ocean, thereby generating a horizontal cell. But the leeward piling up of water is the same in the two cases.

[9] The entire density contrast across the upper ocean basin and thus the net geostrophic transport of upper waters reflects both the contribution from the upper part of deep thermohaline overturning circulation (T_{gt}) and the lower part of the shallower wind driven overturning

$$T_g = T_{gt} + T_{gw} = T_{gt} - T_e\,. \tag{3}$$

Predicted upper ocean geostrophic transport for the Atlantic and Pacific Oceans are shown in Figure 1. The upper limb of the thermohaline overturning circulation, T_{gt} (solid line), is taken as 14 Sv northward for all latitudes in the Atlantic, 8 Sv northward south of the equator in the Pacific feeding the Indonesian throughflow, and 0 Sv north of the equator in the Pacific [*Schmitz*, 1995]. While many ocean general circulation models show that the strength of the thermohaline overturning cell varies considerably with latitude (significant transformation of deep to intermediate and surface waters in low and midlatitudes), interpretations based on observations in the real ocean suggest that strong vertical motions in the thermohaline overturning are restricted to high latitudes, and the strength of upper branch of the thermohaline overturning changes little with latitude in the subtropics and tropics. *Schmitz* [1995] compiles estimates based on several studies and shows that the northward transport in upper and intermediate waters (above a sigma-theta of 27.5) of the Atlantic Ocean is 14 Sv at 32°S, 24°N and just south of the polar seas. Similarly,

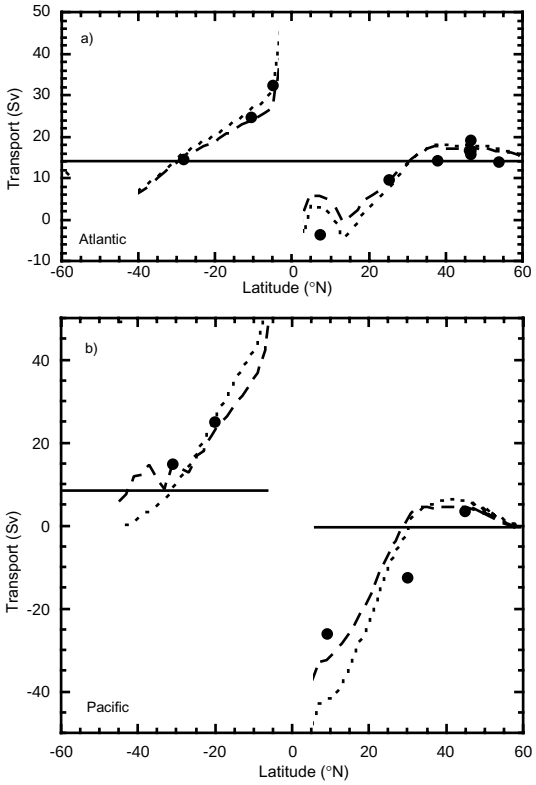

Figure 1. Meridional geostrophic transport (positive northward) in (a) the Atlantic Ocean and (b) the Pacific Ocean. The dashed lines are predicted transport, $T_g = T_{gt} - T_e$. The upper limb of the thermohaline overturning circulation, T_{gt} (solid line), is taken as 14 Sv northward for all latitudes in the Atlantic, 8 Sv northward south of the equator in the Pacific feeding the Indonesian throughflow, and 0 Sv north of the equator in the Pacific. The Ekman transport, T_e, is taken from *Harrison* [1989] (long dashes) and Hellerman and Rosenstein [*Hellerman and Rosenstein*, 1988; *Levitus*, 1988] (short dashes) wind stress climatologies. The solid circles are the upper ocean (0–1000 m) meridional geostrophic transports calculated from the WOCE ocean margin data, where the transport was calculated assuming a 1000 m reference level.

Ganachaud and Wunsch [2000] using the newer WOCE data set also show at the same latitudes 16 ± 3, 16 ± 2 and 14 ± 2 Sv for northward flow above the neutral density surface 27.72. The Ekman transport, T_e, is

taken from the *Harrison* [1989] and Hellerman and Rosenstein [*Hellerman and Rosenstein*, 1988; *Levitus*, 1988] wind stress climatologies.

[10] In general, the Ekman transport (and thus the compensating subsurface geostrophic flow) and the strength of the upper branch of the thermohaline overturning cell are of comparable magnitudes and both must be considered. In the Pacific, where the ocean basin is wider, the transport in the wind driven cells is larger. At higher latitudes, as the Ekman transport becomes smaller (owing to higher Coriolis parameter, f), the transport becomes dominated by the upper branch of the thermohaline overturning circulation.

3. Cross-Basin Transport Calculations From Oceanographic Data

[11] We now use actual temperature and salinity measurements from the ocean margins to test the simple ideas discussed above, which rested on several assumptions. First we assume that reasonable geostrophic transports across the entire width of the ocean basin can be estimated using a single reference level. Detailed hydrographic sections have shown that the meridional motion is not spread smoothly across the ocean basin but shows "patches" or "columns" of several tens of degrees of latitude where the waters contain more of a northward component and adjacent patches with a more predominantly southward flow. There is no single depth across the entire ocean basin where the velocity diminishes to zero. While detailed transport studies across ocean basins using closely spaced CTD stations now typically assign a variable level of no motion between station pairs chosen to satisfy various constraints, earlier studies using a single level of no motion have resulted in reasonable transport calculations. Perhaps this reflects the fact that while there indeed is no strict level of no motion, there are still levels of relatively little motion. When looking at the cross-basin density contrast, our reference level is not really a level of no motion but rather the depth at which the net flow across the entire basin is zero. We first assume a 1000 m reference level for both the Atlantic and Pacific Oceans and explore the sensitivity of our results to this choice.

[12] Second we assume that the wind driven circulation is largely closed within the upper ocean. We will first define the "upper ocean" to be 1000 m but will again explore the sensitivity of our results to this choice. We have also assumed in the above discussion that while nongeostrophic flow is necessary along the western boundary consistent with the observed north–south density contrasts along this margin, that the nongeostrophic portion of the flow is small compared to the magnitude of the offshore flows which are geostrophically balanced.

[13] We used the World Ocean Circulation Experiment (WOCE) data for the Atlantic and Pacific Oceans (http://whpo.ucsd.edu/whp_data.htm, public data only). We used only the CTD data nearest to the ocean margin to construct the best approximation to the temperature and salinity distribution along the margin itself by starting with the shallowest (inshore) CTD cast, then appending to the bottom of this the data from the next shallowest cast until the desired depth (e.g., 1000 m) was reached (Table 1). The net mass transport between two vertical profiles can be calculated from the difference in potential energy anomaly (χ) between the two stations. An analogous potential, Q, can be computed in order to calculate the volume transport [*Sato and Rossby*, 1995; *United*

Table 1. Composite Ocean Margin Profiles

Latitude	Western Profiles			Eastern Profiles			Transport, Sv
	Cruise	Stations	Q, 100 m^3 s^{-2}	Cruise	Stations	Q, 100 m^3 s^{-2}	
				Atlantic			
53.7	AR07W (1990)	24–29, 31	24.3	A01E	618–622	40.8	14
46.2	AR19 (July 1993)	11, 13–16	25.7	AR19 (July 1993)	79–85	42.3	16
46.2	AR19 (1996)	151, 153, 155, 157, 159, 161	23.4	AR19 (1996)	7, 9, 11, 13, 15, 17	43.6	19
46.2	AR19 (1998)	65–70	24.1	AR19 (1998)	2–7	41.6	17
46.2	A02 (1997)	333–337	24.8	A02 (1997)	277–282	42.6	17
37.7	A03	130–133	27.2	A03	3, 4, 6, 7	39.9	14
25.3	A05	100, 101, 106–109, 111, 112	40.8	A05	1–6	46.7	10
7.1	A06	120–124	48.2	A06	198–203	47.5	−3
−5.1	A07	89–91	52.6	A07	1–6	48.5	33
−10.7	A08	169–171	54.8	A08	270–274, 287–290	48.1	25
−18.4	A09	125–126	57.1	A09	232	46.2	24
−28.3	A10	622–628	56.3	A10	96–99	46.2	15
				Pacific			
44.9	P01	1–5	48.2	P01	112–115	51.9	4
30.0	P03	359, 363, 367, 382, 384–387, 389	61.3	P03	2, 3, 6, 16, 18	52.2	−12
8.9	P04W	3–6	59.9	P04E	219–221	54.1	−26
−20.3	P21	286–288	64.7	P21	14–17	52.0	25
−31.3	P06W	243–246	62.0	P06E	4–6	50.6	15

Nations Educational, Scientific and Cultural Organization (UNESCO), 1991],

$$Q = \int_{p_0}^{p} (\eta - z)\,\delta dp, \tag{4}$$

where p is pressure, η is the free surface, z is depth, and δ is the specific volume anomaly. Following [*UNESCO*, 1991] we calculate Q (in 100 m^3 s^{-2}) for each profile (first, relative to 1000 m, later with other reference levels) and then compute the net geostrophic transport (T_g in Sverdrups) between the eastern and western sides of the ocean basin relative to the chosen reference level:

$$T_g = (Q_e - Q_w)/(10^4 f). \tag{5}$$

[14] Note that the potential computed for the eastern margin (Q_e) of each basin is almost constant (Table 1), with most of the north–south variability in the meridional geostrophic transport determined by the changes in potential along the western margin (Q_w). Using a simplified two-layer model for wind driven ocean circulation, *Veronis* [1973] similarly observed that the height of the thermocline was quite constant along the eastern wall of the ocean basin, whereas the variability of thermocline depth along the western wall is significant. He attributes the constant thermocline height on the eastern side of the basin to the requirement for vanishing normal transport at the eastern wall. Because the flows along the eastern boundary are relatively weak, they reflect the geostrophic balance, and thus thermocline height (and in our case, Q) must be constant to reflect the fact that there is no flow into or out of the boundary. The more complex situation along the western boundary allows for a variable thermocline height (and also Q) along that boundary. Here, *Veronis* [1973] calls on the importance of friction and inertial processes near the western boundary that cause a departure from geostrophy. The practical consequence is that in order to characterize the ocean circulation from ocean margin density measurements, we will need many fewer density measurements along the eastern boundary than along the western boundary.

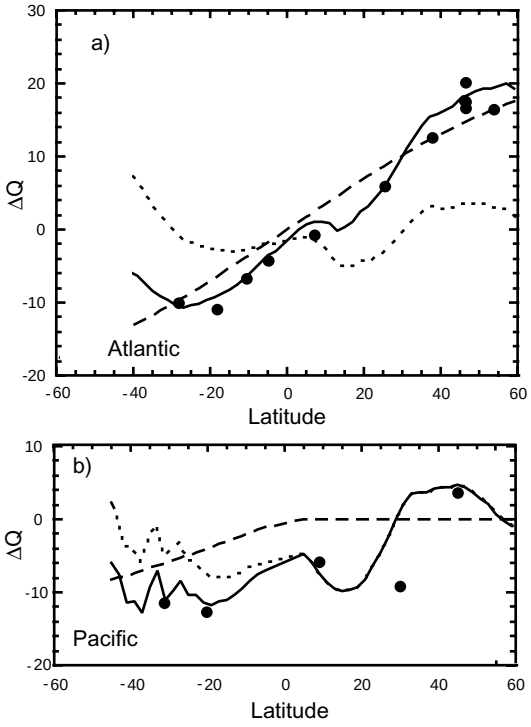

Figure 2. Cross basin gradient in the potential, $\Delta Q = Q_e - Q_w$. Gradient predicted from the wind driven circulation (short dashed line, based on *Harrison* [1989] wind stress climatology), overturning circulation (line with long dashes), and the predicted total gradient, the sum of the above (solid line). The solid circles are is the observed ΔQ referenced to 1000 m.

[15] While the wind driven geostrophic transport is large at low latitudes, we note that the density contrast (as reflected in $Q_e - Q_w$) supporting this contrast is small (Figure 2; equation (4)). The largest (and thus easiest to reconstruct from sediment data) density contrasts will be at high latitudes, supporting the thermohaline overturning circulation. This results from the fact that for a constant trans-

port, $Q_e - Q_w$ must increase as f increases at high latitudes.

[16] Choosing a reference level at 1000 m, the calculated contrast in Q and transport derived from the WOCE ocean margin data agrees well with that predicted from the Ekman transport and the thermohaline circulation estimates of *Schmitz* [1995] (Figures 1 and 2). The agreement is poorer for the Pacific Ocean than for the Atlantic Ocean, which is not surprising given both the more complex geometry of the western margin of the Pacific Ocean, the higher uncertainties in the magnitude of the thermohaline and wind driven circulation used for the predicted transport, and the large interannual variability of the Pacific winds which is reflected in the WOCE data but not the wind stress climatologies upon which the predicted transport is based. For the Pacific Ocean, the calculated meridional geostrophic transport is relatively insensitive to the choice of level of reference level (Figure 3). This reflects the fact that the vertical shear in the thermohaline overturning circulation is very small below 1000 m, and the effects of the wind driven circulation are also greatly diminished by this depth. However, in the Atlantic Ocean where the shear in the overturning circulation is large (strong "conveyor"), the calculation transport is very sensitive to the choice of reference level. However, the difference in transport from one latitude to the next, which reflects primarily the strength of the winds, is relatively insensitive to the choice of reference level. The same conclusion was reached by *Roemmich* [1983] who found that the divergences in geostrophic transport between sections in the tropical Atlantic Ocean matched the Ekman convergences calculated from wind data. *Roemmich* [1983] also argued that the upper layer (wind driven) transports were relatively insensitive to the choice of reference for his geostrophic calculations. This reflects the fact that the effect of the wind on ocean circulation diminishes with depth.

4. Application for Paleoceanographic Reconstruction

4.1. Density From $\delta^{18}O$ in Foraminifera

[17] We can use the $\delta^{18}O$ from the calcite tests of benthic foraminifera preserved in ocean sediments to estimate upper ocean density on the ocean margins because both the $\delta^{18}O$ of calcite ($\delta^{18}O_{calcite}$) and density increase as a result of increasing salinity or decreasing temperature [*Lynch-Stieglitz et al.*, 1999a] (Figure 4). The fractionation between calcite precipitated inorganically and the water in which it forms increases by ~0.2‰ for every 1°C decrease in temperature [*Kim and O'Neil*, 1997], and the isotopic composition of calcitic benthic foraminifera in the genera *Planulina* and *Cibicidoides* shows the same fractionation as measured in the experiments with inorganic calcite [*Lynch-Stieglitz et al.*, 1999a]. The relationship between $\delta^{18}O_{calcite}$ and salinity is more complex. The $\delta^{18}O_{calcite}$ reflects the $\delta^{18}O$ of the water in which the foraminifera grew. The $\delta^{18}O$ of seawater ($\delta^{18}O_{water}$) primarily reflects patterns of evaporation and freshwater influx to the surface of the ocean. Because salinity also reflects these same processes, salinity and $\delta^{18}O_{water}$ are often well correlated in the ocean. Although the exact relationship varies in different areas of the surface ocean [*Craig and Gordon*, 1965], the vast majority of surface and warm subsurface waters ($T > 5$°C) in the ocean have salinity and $\delta^{18}O_{water}$ values which scatter around a linear trend [*Lynch-Stieglitz et al.*, 1999a].

[18] For times in the geologic past, our ability to reconstruct density from the $\delta^{18}O_{calcite}$ is most limited by our knowledge of the relationships between $\delta^{18}O_{water}$ and salinity, as well as the relationships between temperature and sal-

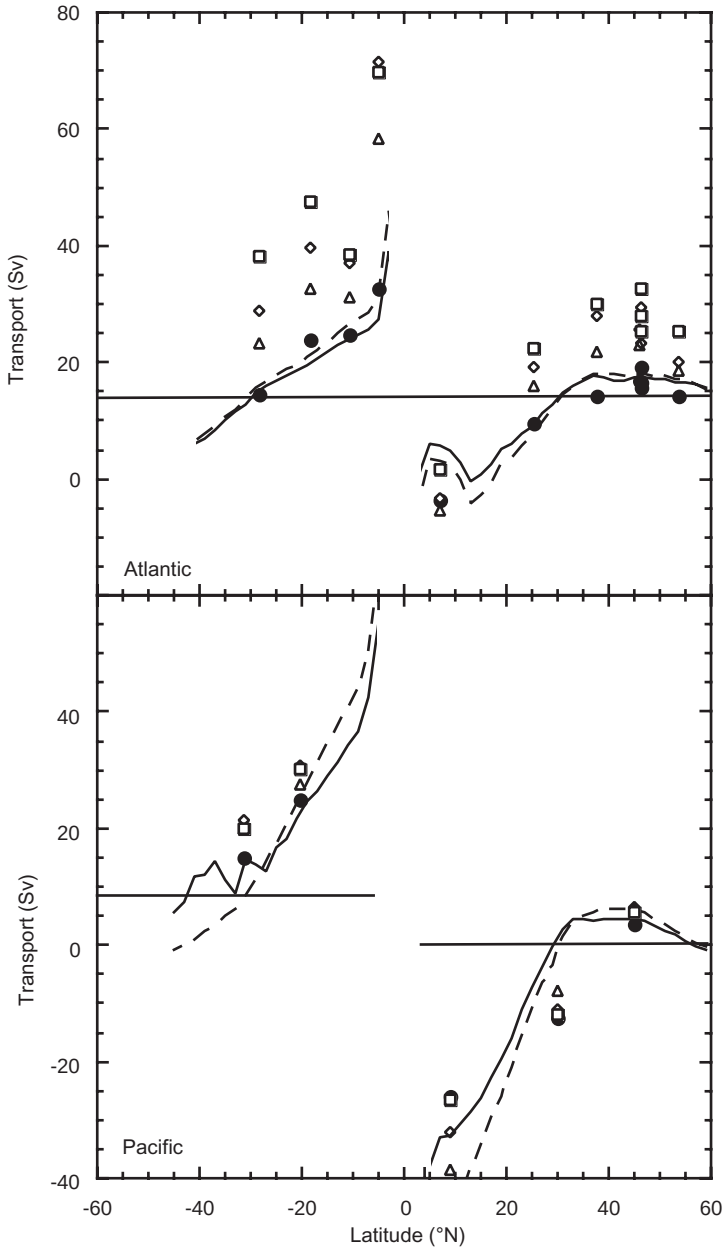

Figure 3. Sensitivity of meridional geostrophic transport to reference level. Transports are calculated for the upper ocean (surface to reference level) using reference levels of 1000 (solid circle), 1300 (triangle), 1500 (diamond), and 2000 m (square). Predicted transport (dashed lines) is shown as in Figure 1.

inity. By taking into consideration the presumed changes in ocean salinity and $\delta^{18}O_{water}$ due to sea level change and possible changes in the $\delta^{18}O$ of high latitude precipitation, we can make an educated guess about the relationship between $\delta^{18}O_{water}$ and salinity for the past ocean and determine the relationship between $\delta^{18}O_{calcite}$ and density [*Lynch-Stieglitz et al.*,

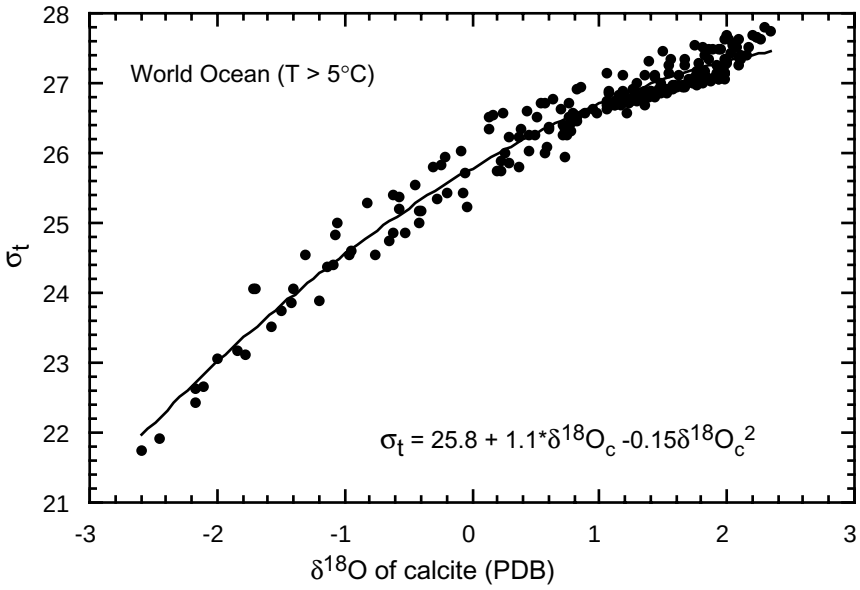

Figure 4. Density anomaly (sigma-T) versus $\delta^{18}O_{calcite}$ relationship for today's warm ocean ($T > 5°C$). Temperature, salinity, and $\delta^{18}O_{water}$ data are from open ocean GEOSECS stations in all three ocean basins where $T > 5°C$. The isotopic composition of foraminiferal calcite for these upper waters is calculated using the GEOSECS $\delta^{18}O_{water}$ and temperature data, and the *Planulina* and *Cibicidoides* based paleotemperature equation [*Lynch-Stieglitz et al.*, 1999a]. The density is calculated using the temperature and salinity data from the sample locations. The scatter in this relationship mainly results from regional variability in the T-S-$\delta^{18}O_{water}$ relationship. The relationship between sigma-T and $\delta^{18}O_{calcite}$ for individual ocean basins contain much less scatter [*Lynch-Stieglitz et al.*, 1999a].

1999b; *Lynch-Stieglitz et al.*, 1999c]. The upper ocean cross basin density contrasts translate into $\delta^{18}O$ differences in the foraminifera at a given depth of more than 0.5‰ (Figure 5). This signal can be well resolved for paleoceanographic applications.

[19] While we have shown that we can reconstruct ocean margin density in the upper ocean, deep ocean density contrasts would be equally useful for constraining the overturning circulation of the ocean. At high latitudes the relationship between $\delta^{18}O_{water}$ and salinity becomes far more complex because, in addition to evaporation and precipitation, sea ice formation causes salinity and $\delta^{18}O_{water}$ changes. However, the fractionation of oxygen isotopes during ice formation is much smaller than during evaporation. This would make a detailed reconstruction of density from $\delta^{18}O_{calcite}$ in high latitude surface water difficult without additional information. However, deep waters are formed in only a few places in the world, resulting in a good correlation of $\delta^{18}O_{water}$ and salinity in deep waters today (although different from the upper ocean correlation) [*Broecker*, 1986; *Craig and Gordon*, 1965]. It is possible that this relationship could be deduced for the last glacial maximum from the $\delta^{18}O_{water}$ and salinity signal preserved in pore waters [*Adkins and Schrag*, 2001; *Schrag et al.*, 1996]. If this problem were surmounted, we would then have to examine whether foraminifera can accurately record the very subtle gradients in $\delta^{18}O_{calcite}$ from deep waters. For example, at 30°S in the Atlantic Ocean the cross-basin temperature contrast at

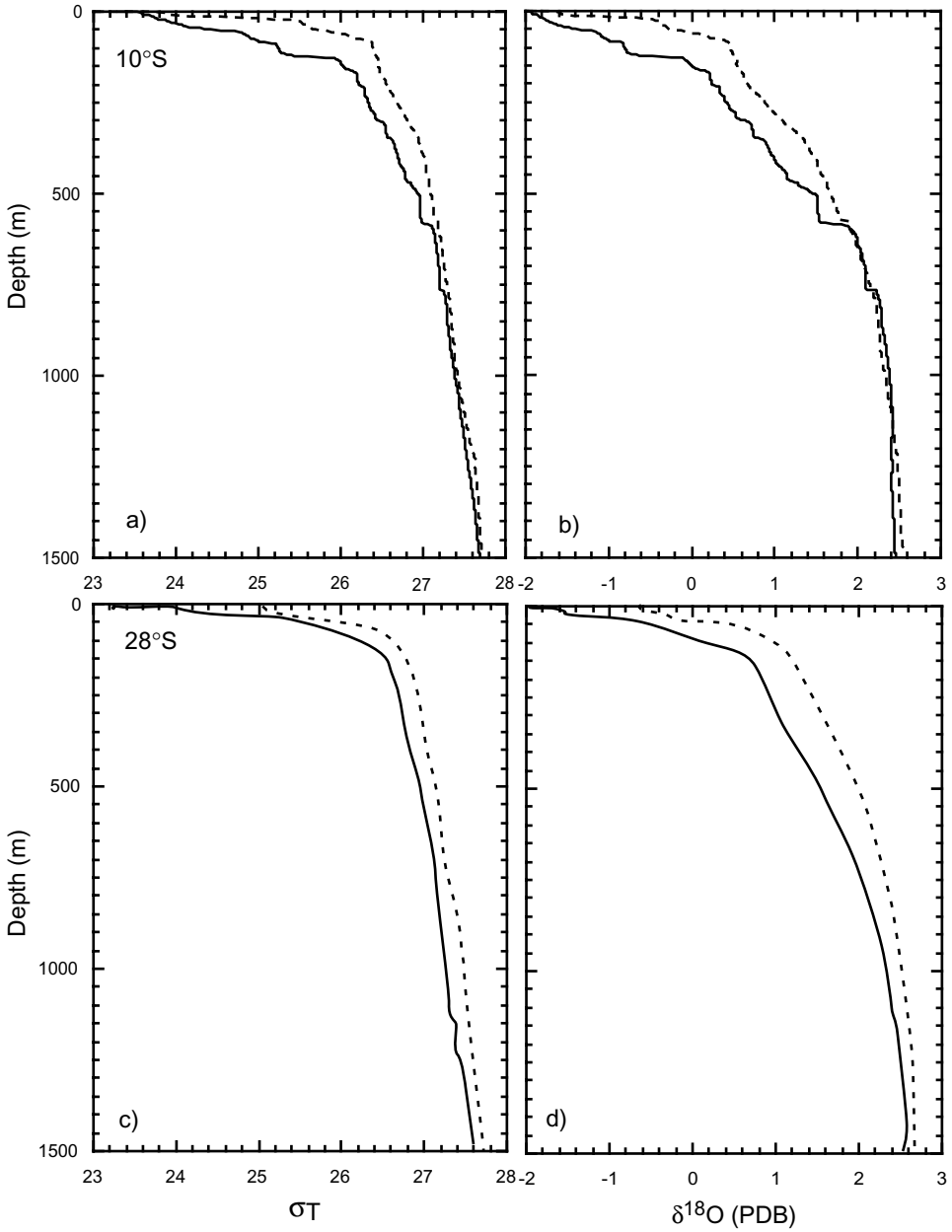

Figure 5. (a) Density anomaly and (b) $\delta^{18}O_{calcite}$ profiles along the western (solid lines) and eastern (dashed lines) margin of the Atlantic Ocean at 10°S. The large wind driven geostrophic transport at this latitude is supported by large density contrast in the upper 600 m. (c) Density anomaly and (d) $\delta^{18}O_{calcite}$ profiles along the western (solid lines) and eastern (dashed lines) margin of the Atlantic Ocean at 28°S. The shear in the meridional overturning circulation is supported by an east–west density contrast throughout the upper water column.

3000 m is 0.9°C and that for salinity is −0.09‰. This would result in a $\delta^{18}O_{calcite}$ contrast of less than 0.1‰, close to the analytical error on the isotope measurements. At this point in time, we are much more likely to be able to obtain useful density reconstructions from the upper ocean.

[20] The spatial resolution of ocean margin density estimates will also ultimately limit the utility of this method in deducing past ocean circulation. Not all locations along the ocean margins have continuous deposition of sediments or sufficient abundances of benthic foraminifera to allow reconstructions for all time periods at all time resolutions. While it would be ideal to collect a depth transect of cores along a fixed latitude (especially for the western boundary), appropriate sediment deposits may span a limited latitude range. Detailed interpretations of density reconstructions will also require strict time control for all cores used in the study, as well as careful attention to intercalibration of oxygen isotope measurements between laboratories. While existing sediment cores will provide some ocean margin density information, detailed reconstructions of flow even for the Last Glacial Maximum will require targeted coring of ocean margin sediments.

4.2. Inferences From Referenced Transport Calculations

[21] We have shown above (Figure 1) that if we use an appropriate reference level, the net meridional geostrophic transport of upper waters can be calculated from paired profiles of upper ocean density. For a time in the past, such as the Last Glacial Maximum, we could reconstruct such a profile by using a vertical transect of sediment cores on either side of the ocean basin and measuring the $\delta^{18}O_{calcite}$ of the benthic foraminifera from the glacial levels in these cores. As mentioned above, we can take advantage of the fact that the density, and thus Q, is relatively constant from north to south along the eastern margin and need only construct vertical profiles at a few places along the eastern margin. Today, the zonal winds change direction within a few degrees latitude of 30°N and 30°S for all ocean basins. If we assume that this was also the case in the past, we could determine the strength of the upper branch of the thermohaline overturning circulation by combining our eastern margin density information with vertical density profiles from the western margin at 30°N and 30°S. Once we have determined the strength of the thermohaline circulation, we could then determine the average strength of the zonal winds using vertical profiles at other latitudes by subtracting this component from the total transport. This requires the assumption that like today, the strength of the thermohaline-overturning cell varies little within the tropics and subtropics. As long as we choose a reference level below 1000 m or so, the calculation of zonal winds is relatively robust. However, the calculation of the magnitude of the thermohaline overturning circulation depends strongly on the chosen reference level.

[22] What is the best way to determine the appropriate reference level for times in the past? If we could accurately reconstruct density in deep waters, we could impose a reference level using the constraint that the same amount of water must travel northward across each section as is transported to the south. However, this would require an accurate reconstruction of the very subtle density gradients in deep water (not realistic at this time). Another possibility is to let the nutrient tracer (carbon isotope and trace metal) distributions inferred for the past ocean help determine water mass boundaries and thus an appropriate reference level. For example, if it appeared that the boundary between southward flowing NADW and northward penetrating Antarctic Intermediate Water

shoaled in the South Atlantic, it might be appropriate to choose a shallower reference level. However, here too it is difficult to imagine at this time the nutrient distributions yielding precise enough information about water mass movements to constrain the reference level to a useful degree (approximately ±100 m). Sedimentary grain size has been used to determine qualitatively bottom water flow strength, with coarser grained deposits underlying faster currents [e.g., *Bulfinch et al.*, 1982; *McCave et al.*, 1995]. A vertical transect of grain size along the western boundary where currents are intensified could be used to determine the depth of the weakest flows, which could be used as a reference level across the section. However, in the face of the difficulty in determining an appropriate reference level for times in the past, combined with the sensitivity of any calculations of the absolute strength of upper ocean transport to such a choice, it is perhaps wisest to simply be satisfied with using the density contrast to establish the shear in the overturning circulation as well as the absolute strength of the zonal winds (which is less sensitive to reference level choice).

4.3. Model Validation

[23] Additional insights into the circulation of past oceans could be gained by using ocean margin density information in conjunction with numerical models of ocean circulation. Any realistic simulation of past ocean circulation should be broadly consistent with observed ocean margin density structure. Deficiencies in the wind field driving the model, surface processes in high latitudes where upper waters are formed, and the large-scale overturning circulation of the ocean will all contribute to mismatches between observed and modeled ocean margin densities. Ocean margin density data could also be used as an additional constraint actively imposed on a model of past ocean circulation.

5. Conclusions

[24] The best reconstructions of paleoocean flow are based on (1) using reconstructed ocean surface properties to drive dynamic models of ocean circulation and (2) using the distribution of nutrient tracers in the deep ocean to infer deep flow and to validate the ocean circulation model results. Here we show that the density along the ocean margins contains important information about both the strength of the zonal winds over the ocean (and the resulting wind driven circulation) and the shear in the meridional overturning associated with the thermohaline circulation. The density gradients along the margins are large in the upper ocean and are well resolved in the oxygen isotopic composition of benthic foraminifera. We propose that both geographically targeted and large-scale reconstruction of ocean margin density will provide an important third constraint for the reconstruction of paleocean circulation. Estimates of zonal average surface wind strength over the oceans will also provide an important constraint for reconstructing atmospheric circulation. It has been suggested that the increased equator to pole temperature gradients during the last glaciation resulted in stronger winds. However, paleoceanographic reconstructions of upwelling strength [e.g., *Pedersen and Bertrand*, 2000; *Sarnthein et al.*, 1988], aeolian grain size [e.g., *Hesse and McTainsh*, 1999; *Petit et al.*, 1981; *Rea*, 1994] and thermocline structure [*Andreasen and Ravelo*, 1997] do not yet present a coherent picture of high glacial winds.

Acknowledgments

[25] I thank George Veronis, Martin Visbeck, Tom Marchitto, Gidon Eshel, Dan Schrag, and an anonymous reviewer for their comments which improved the manuscript substantially. A discussion with Carl Wunsch also helped to clarify my thinking. I also thank Christopher Gorski who did some initial work on this topic for his undergraduate summer internship. This

work was supported by NSF CAREER Award OCE 99-84989.

References

Adkins, J., and D. Schrag, Pore fluid constraints on deep ocean temperature and salinity during the last glacial maximum, *Geophys. Res. Lett.*, *28*, 771–774, 2001.

Andreasen, D. J., and A. C. Ravelo, Tropical Pacific Ocean thermocline depth reconstructions for the Last Glacial Maximum, *Paleoceanography*, *12*, 395–413, 1997.

Broecker, W. S., Oxygen isotope constraints on surface ocean temperatures, *Quat. Res.*, *26*, 121–134, 1986.

Bulfinch, D., M. Ledbetter, B. Ellwood, and W. Balsam, The high-velocity core of the western boundary undercurrent at the base of the United States continental rise, *Science*, *215*, 970–973, 1982.

Craig, H., and L. I. Gordon, Deuterium and oxygen 18 variations in the ocean and the marine atmosphere: Stable isotopes in oceanographic studies and paleotemperatures, in *Proceedings of the Third Spoleto Conference, Spoleto, Italy*, edited by E. Tongiori, pp. 9–130, Sischi and Figli, Pisa, Italy, 1965.

Curry, R., and M. McCartney, Ocean gyre circulation changes associated with the North Atlantic Oscillation, *J. Phys. Oceanogr.*, in press, 2001.

Ganachaud, A., and C. Wunsch, Improved estimates of global ocean circulation, heat transport and mixing from hydrographic data, *Nature*, *408*, 453–457, 2000.

Harrison, D. E., On climatological monthly mean wind stress and wind stress curl fields over the World Ocean, *J. Clim.*, *2*, 57–70, 1989.

Hellerman, S., and M. Rosenstein, Normal monthly wind stress over the World Ocean with error estimates, *J. Phys. Oceanogr.*, *13*, 1093–1104, 1988.

Hesse, P., and G. McTainsh, Last Glacial Maximum to Early Holocene wind strength in the mid-latitudes of the Southern Hemisphere from aeolian dust in the Tasman Sea, *Quat. Res.*, *52*, 343–349, 1999.

Kim, S. T., and J. R. O'Neil, Equilibrium and nonequilibrium oxygen isotope effects in synthetic carbonates, *Geochim. Cosmochim. Acta*, *61*, 3461–3475, 1997.

Levitus, S., Ekman volume fluxes for the World Ocean and individual ocean basins, *J. Phys. Oceanogr.*, *18*, 271–279, 1988.

Lynch-Stieglitz, J., W. Curry, and N. Slowey, A geostrophic transport estimate for the Florida Current from oxygen isotope composition of benthic foraminifera, *Paleoceanography*, *14*, 360–373, 1999a.

Lynch-Stieglitz, J., W. Curry, N. Slowey, and G. Schmidt, The overturning circulation of the glacial Atlantic: A view from the top, in *Reconstructing Ocean History: A Window into the Future*, edited by F. Abrantes, and A. Mix, pp. 7–31, Plenum, New York, 1999b.

Lynch-Stieglitz, J., W. B. Curry, and N. Slowey, Weaker Gulf Stream in the Florida Straits during the Last Glacial Maximum, *Nature*, *402*, 644–648, 1999c.

Marotzke, J., R. Giering, K. Zhang, D. Stammer, C. Hill, and T. Lee, Construction of the adjoint MIT ocean general circulation model and application to Atlantic heat transport sensitivity, *J. Geophys. Res.*, *104*, 29,529–29,547, 1999.

McCave, I., B. Manighetti, and S. G. Robinson, Sortable silt and fine sediment size/composition silicing: Parameters for palaeocurrent speed and palaeoceanography, *Paleoceanography*, *10*, 593–610, 1995.

McCreary, J. P., and P. Lu, Interaction between the subtropical and equatorial ocean circulations: The subtropical cell, *J. Phys. Oceanogr.*, *24*, 466–497, 1994.

Pedersen, T., and P. Bertrand, Influences of oceanic rheostats and amplifiers on atmospheric CO2 content during the Late Quaternary, *Quat. Sci. Rev.*, *19*, 273–283, 2000.

Petit, J., M. Briat, and A. Royer, Ice age aerosol content from East Antarctic ice core samples and past wind strength, *Nature*, *293*, 391–394, 1981.

Rea, D. K., The paleoclimatic record provided by eolian deposition in the deep sea: The geologic history of wind, *Rev. Geophys.*, *32*, 159–195, 1994.

Roemmich, D., The balance of geostrophic and Ekman transports in the Tropical Atlantic Ocean, *J. Phys. Oceanogr.*, *13*, 1534–1539, 1983.

Sarnthein, M., K. Winn, J.-C. Duplessy, and M. Fontugne, Global variations of surface ocean productivity in low and mid latitudes: Influence on CO_2 reservoirs of the deep ocean and atmosphere during the last 21,000 years, *Paleoceanography*, *3*, 361–399, 1988.

Sato, O. T., and T. Rossby, Seasonal and low frequency variations in dynamic height anomaly and transport of the Gulf Stream, *Deep Sea Res. Part I.*, *42*, 149–164, 1995.

Schmitz, W. J., On the Interbasin-scale thermohaline circulation, *Rev. Geophys.*, *33*, 151–173, 1995.

Schrag, D. P., G. Hampt, and D. W. Murray, Pore fluid constraints on the temperature and oxygen isotopic composition of the glacial ocean, *Science*, *272*, 1930–1932, 1996.

United Nations Educational, Scientific and Cultural Organization, (UNESCO), *Processing of Oceanographic Station Data*, 138 pp., Joint Program on Oceanogr. Tables and Stand, Paris, 1991.

Veronis, G., Model of the world ocean circulation, I, Wind-driven, two layer, *J. Mar. Res.*, *31*, 228–288, 1973.

Veronis, G., Dynamics of large-scale ocean circulation, in *Evolution of Physical Oceanography: Scientific Surveys in Honor of Henry Stommel*, edited by B. A. Warren, and C. Wunsch, pp. 140–183, MIT Press, Cambridge, Mass., 1981.

Whitworth, T., Monitoring the transport of the Antarctic Circumpolar Current at Drake Passage, *J. Phys. Oceanogr.*, *11*, 2045–2057, 1983.